Molecular Therapy
Nucleic Acids
Original Article

Lnc-CCNH-8 promotes immune escape by up-regulating PD-L1 in hepatocellular carcinoma

Bixing Zhao,[1,2,3,4] Xiaoyuan Zheng,[1,2,3,4] Yang Wang,[1,2,4] Niangmei Cheng,[1,2,3,4] Yue Zhong,[1] Yang Zhou,[1,2,3] Jingyun Huang,[1,2] Fei Wang,[1,2,3] Xin Qi,[1,2] Qiuyu Zhuang,[1,2,3] Yingchao Wang,[1,2,3] and Xiaolong Liu[1,2,3]

[1]The United Innovation of Mengchao Hepatobiliary Technology Key Laboratory of Fujian Province, Mengchao Hepatobiliary Hospital of Fujian Medical University, Fuzhou 350025, P.R. China; [2]Mengchao Med-X Center, Fuzhou University, Fuzhou 350116, P.R. China; [3]Fujian Provincial Clinical Research Center for Hepatobiliary and Pancreatic Tumors, Fuzhou 350025, P.R. China

Hepatocellular carcinoma (HCC) is a common malignancy with poor prognosis. In recent years, immune checkpoint inhibitors (ICIs) have enabled breakthroughs in the clinical treatment of patients with HCC, but the overall response rate to ICIs in HCC patients is still low, and no validated biomarker is available to guide clinical decision making. Here, we demonstrated that the long non-coding RNA Lnc-CCNH-8 is highly expressed in HCC and correlates with poor prognosis. Functionally, elevated Lnc-CCNH-8 inactivated co-cultured T cells *in vitro* and compromised antitumor immunity in an immunocompetent mouse model. Mechanistically, up-regulated Lnc-CCNH-8 can sponge microRNA (miR)-217 to regulate the expression of PD-L1. In addition, Lnc-CCNH-8 can also stabilize PD-L1 through miR-3173/PKP3 axis. Furthermore, mice bearing tumors with high Lnc-CCNH-8 expression had significant therapeutic sensitivity to anti-PD-L1 monoclonal antibody treatment. More important, HCC patients with high levels of plasma exosomal Lnc-CCNH-8 had a better therapeutic response to ICIs. Taken together, our results reveal the function of Lnc-CCNH-8 in inducing immune escape from $CD8^+$ T-cell-mediated killing by up-regulating PD-L1 in a miR-217/miR-3173-dependent manner, which also reveals a novel mechanism of PD-L1 regulation in HCC, and exosomal Lnc-CCNH-8 can serve as a predictive marker for immunotherapy response in HCC.

INTRODUCTION

Hepatocellular carcinoma (HCC) is the sixth most common malignancy worldwide and the third leading cause of cancer-related death.[1] In recent years, surgical and locoregional therapies for HCC have made remarkable progress, but the overall prognosis of HCC patients is still unsatisfactory. Exploring novel effective therapeutic targets is essential for the improvement of therapeutic outcomes.

Programmed death-ligand 1 (PD-L1) on cancer cells engages with programmed cell death-1 (PD-1) on immune cells, contributing to cancer immune escape. For multiple cancer types, the PD-1/PD-L1 axis is the most important speed-limiting step of the anti-cancer immune response. PD-L1 is highly expressed in a variety of tumor cells, and its expression is precisely regulated at multiple levels, including genomic alterations, epigenetic modification, transcriptional, post-transcriptional modification, and post-translational modification. IFN-γ is the main stimulatory signal to induce PD-L1 expression, mainly through the JAK/STAT signaling pathway at the transcriptional level.[2] At the post-transcriptional modification level, PD-L1 levels are mainly regulated by microRNAs (miRs). For example, miR-513,[3] miR-570,[4] miR-34a,[5] miR-200.[6] and miR-217[7] were all able to directly target and inhibit the expression of PD-L1. In addition, PD-L1 expression is also regulated by long non-coding RNAs (lncRNAs). The LncRNA UCA1 repressed miR-26a/b, miR-193a, and miR-214 expression through direct interaction and then up-regulated the expression of PD-L1 and contributed to the immune escape of gastric cancer cells.[8] Although lncRNAs participate in regulating the expression of PD-L1 in a variety of tumors, how lncRNAs are involved in the regulation of PD-L1 expression and immune escape remains to be further investigated. In addition, evaluating the clinical value of peripheral blood lncRNAs in predicting the prognosis and immune landscape of HCC is of great significance for clinical precision treatment.

In the past few years, immune checkpoint inhibitors (ICIs), represented by anti-PD-1 and anti-PD-L1 antibodies, have enabled breakthroughs in the clinical treatment of patients with HCC. The combination of atezolizumab (an anti-PD-L1 antibody) and the anti-VEGFA antibody

Received 22 April 2023; accepted 18 January 2024;
https://doi.org/10.1016/j.omtn.2024.102125.

[4]These authors contributed equally

Correspondence: Yingchao Wang, The United Innovation of Mengchao Hepatobiliary Technology Key Laboratory of Fujian Province, Mengchao Hepatobiliary Hospital of Fujian Medical University, Fuzhou 350025, P.R. China.
E-mail: yingchaowang@live.com
Correspondence: Xiaolong Liu, The United Innovation of Mengchao Hepatobiliary Technology Key Laboratory of Fujian Province, Mengchao Hepatobiliary Hospital of Fujian Medical University, Fuzhou 350025, P.R. China.
E-mail: xiaoloong.liu@gmail.com

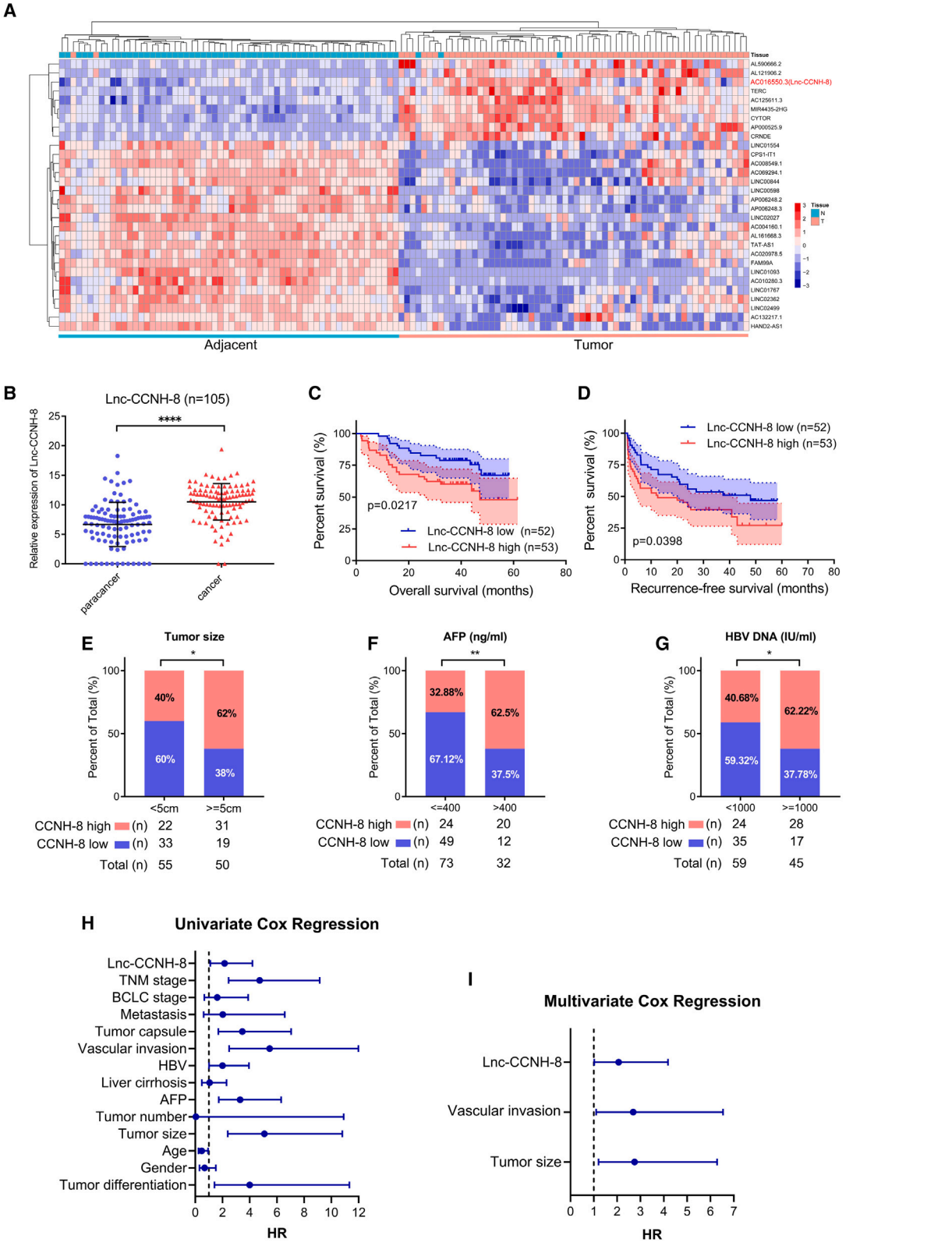

(legend on next page)

bevacizumab has shown superior results compared with sorafenib in patients with advanced-stage HCC,[9] leading to US Food and Drug Administration (FDA) approval of this regimen as first-line therapy. Several large-scale phase III clinical trials of ICI-based combination regimens are currently under way. However, despite these major advances, the response rate of HCC to ICI monotherapy is less than 20% because of the complex pathogenesis of HCC and the immunosuppressive tumor microenvironment.[10] In addition, those who initially respond to ICIs may develop resistance. Thus, on one hand, exploring the molecular basis of immune responses and evasion and designing rational PD-1/PD-L1-based combination therapy have become key to further improving the efficacy of immunotherapy in HCC. On the other hand, the identification of biomarkers that predict the efficacy of PD-1/PD-L1 inhibitors is crucial for patient selection. PD-L1 expression, cytotoxic T lymphocyte infiltration, and tumor mutation burden (TMB) are generally considered to be the most important factors influencing the efficacy of PD-1/PD-L1 blockade.[11] However, no validated biomarker is yet available to guide clinical decision making in HCC. Therefore, it is crucial to find more effective biomarkers for the evaluation of ICI efficacy in HCC.

In the present study, in order to find new immune-related lncRNAs in HCC, high-throughput sequencing and qPCR verification were performed in HCC tissue samples. We show that the lncRNA Lnc-CCNH-8 was significantly up-regulated in HCC and correlated with poor prognosis, and high expression of Lnc-CCNH-8 resulted in induction of PD-L1 expression and increased immune escape of HCC. In addition, mice bearing tumors with high Lnc-CCNH-8 expression showed significant therapeutic sensitivity to PD-L1 monoclonal antibody (mAb) treatment. More important, exosomal Lnc-CCNH-8 can serve as a predictive marker for immunotherapy response in HCC. Taken together, these data demonstrate that Lnc-CCNH-8 may serve as a novel therapeutic target and predictive biomarker in HCC immunotherapy.

RESULTS

Lnc-CCNH-8 was up-regulated in HCC tissues and associated with poor prognosis

LncRNAs have been implicated in the tumorigenesis and progression of cancers, while it remains poorly understood whether lncRNAs can affect tumor immunity. To explore unknown regulatory lncRNAs in tumor immunity, a transcriptome sequencing analysis was performed on 61 pairs of HCC and adjacent non-tumor tissues to identify the differentially expressed lncRNAs (Figure S1). As shown in Figure 1A, among the top 30 differentially expressed lncRNAs, 9 lncRNAs were up-regulated and 21 lncRNAs were down-regulated. Among these lncRNAs, AC016550.3 (Lnc-CCNH-8), which has not been studied before, attracts our attention. The expression levels of Lnc-CCNH-8 were validated using qRT-PCR in a large cohort of 105 pairs of HCC tissues and corresponding adjacent non-tumor tissues. Consistently, the expression of Lnc-CCNH-8 was up-regulated in HCC (Figure 1B). We then investigated the clinicopathological role of Lnc-CCNH-8 and found that higher Lnc-CCNH-8 expression was significantly associated with tumor size, AFP, and hepatitis B virus (HBV) DNA (Figures 1E–1G; Table S1). We further investigated the association between Lnc-CCNH-8 and survival among HCC patients with follow-up data using Kaplan-Meier analysis and log rank test. The results indicated that HCC patients with higher Lnc-CCNH-8 level had a poor overall survival and recurrence-free survival, suggesting that Lnc-CCNH-8 has a potential oncogenic role in HCC (Figures 1C and 1D). Univariate and multivariate analyses further demonstrated that Lnc-CCNH-8 expression was an important prognostic factor for HCC patients (Figures 1H and 1I). Collectively, these results demonstrated that Lnc-CCNH-8 was up-regulated in HCC and that high expression of Lnc-CCNH-8 was associated with poor outcome in HCC.

Lnc-CCNH-8 promotes tumor growth in immunocompetent mice but not in immunodeficient mice

The above clinicopathological analysis data indicated that the expression of Lnc-CCNH-8 was related to tumor size, thus we suspected that Lnc-CCNH-8 might be involved in the growth of HCC. To verify this assumption, the expression of Lnc-CCNH-8 was first detected in various HCC cells (Figure 2A), and then Lnc-CCNH-8 was overexpressed in SK-Hep-1 cells and knocked down in SMMC-7721 cells (Figure S2). The colony formation assay showed that Lnc-CCNH-8 did not affect the colony formation of HCC cells (Figures 2B and S3). The results of the CCK-8 and EdU assays also indicated that Lnc-CCNH-8 was unable to regulate the proliferation of HCC cells (Figures 2C, 2D, S4, and S5). The subcutaneous xenograft tumor model also shows that Lnc-CCNH-8 does not affect the growth of tumor (Figure 2E). Next, we further overexpressed Lnc-CCNH-8 in mouse HCC cell line Hepa1-6 (Figure S2). The subcutaneous murine tumor model was established in both immunodeficient (B-NDG) and immunocompetent (C57/BL6) mice. Interestingly, Lnc-CCNH-8 significantly promoted tumor growth in immunocompetent mice (Figure 2G) but not in immunodeficient mice (Figure 2F). However, in the cell phenotype experiment, Lnc-CCNH-8 also did not affect the proliferation, colony formation, and survival of Hepa1-6 cells (Figures S3, S4, and S6), suggesting that Lnc-CCNH-8 may be involved in the immune escape of HCC.

PD-L1 is a novel downstream target of lnc-CCNH-8 in HCC

To further explore how Lnc-CCNH-8 regulates immune escape of HCC, transcriptional sequencing was performed in control and

Figure 1. Lnc-CCNH-8 was overexpressed in HCC and associated with poor prognosis

(A) Heatmap of the most differentially expressed lncRNA between 61 paired HCC tumor and adjacent normal tissues. (B) qRT-PCR validation of Lnc-CCNH-8 expression in a cohort of HCC patients (n = 105) with paired tumor and para-tumor tissues. 18S rRNA was used as endogenous control. (C and D) Kaplan-Meier analysis of the correlation between Lnc-CCNH-8 expression and overall survival (C) and recurrence-free survival (D) in the cohort of 105 HCC patients. (E–G) Correlation analysis between Lnc-CCNH-8 expression and tumor size (E), AFP (F), and HBV DNA (G). (H and I) Univariate (H) and multivariate (I) Cox regression analysis revealed that Lnc-CCNH-8 expression could be considered as an independent risk factor associated with overall survival among HCC patients.

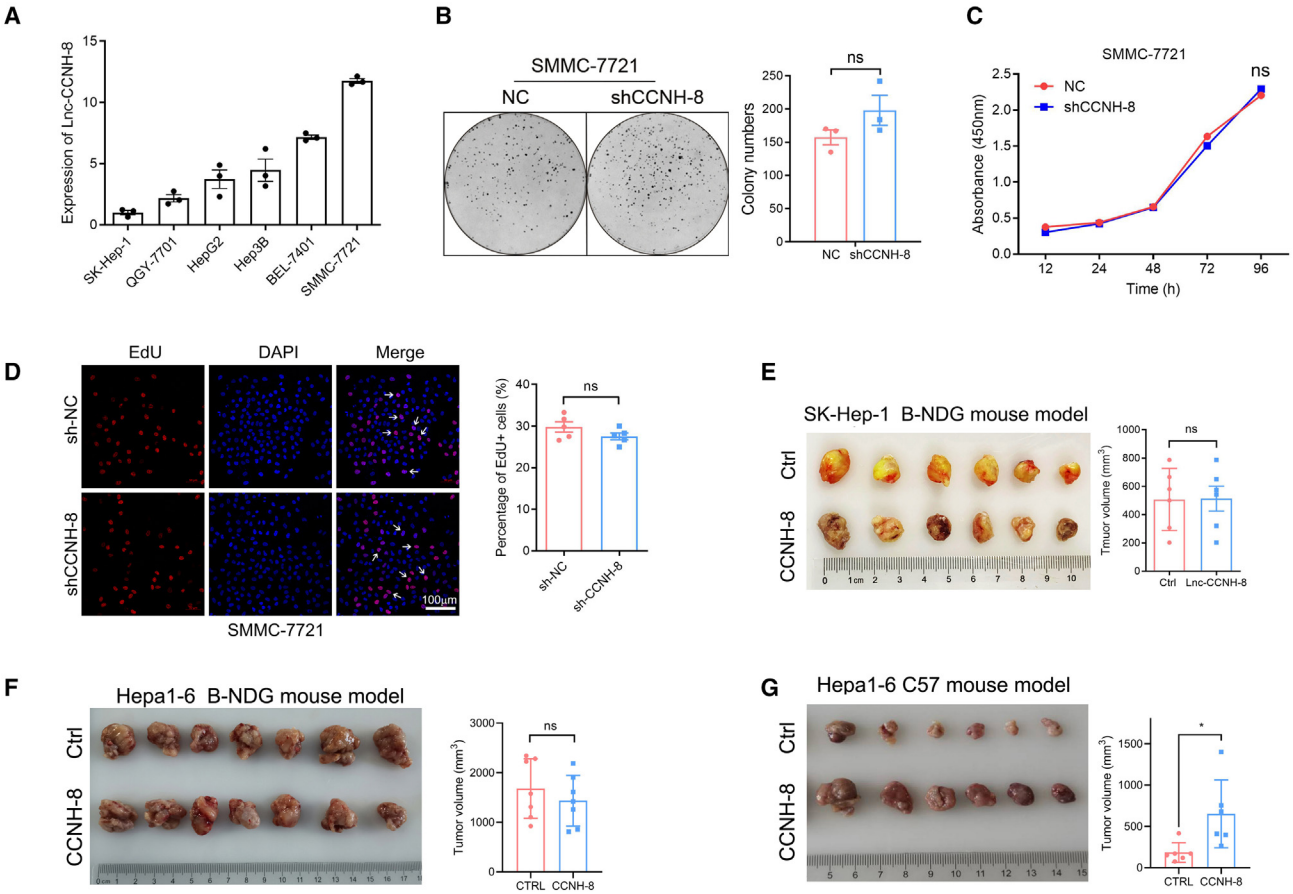

Figure 2. Overexpression of Lnc-CCNH-8 did not affect HCC proliferation in the absence of immunity

(A) Relative expression of Lnc-CCNH-8 in different HCC cell lines. Data are mean ± SEM (n = 3). (B and C) Viability and colony formation of SMMC-7721 cells were evaluated by colony formation assays and CCK-8. (D) EdU proliferation assays for Lnc-CCNH-8 knockdown SMMC-7721 cells (E) The image of tumor size in B-NDG mice injected with control (Ctrl) or Lnc-CCNH-8-overexpressed SK-Hep-1 cells. (F) A picture (left) of xenografts in B-NDG mice injected with Ctrl or Lnc-CCNH-8-overexpressed Hepa1-6 cells. The tumor weight of each group (right). (G) Pictures (left) of xenografts in C57BL/6 mice injected with Ctrl or Lnc-CCNH-8 overexpressing Hepa1-6 cells. The tumor volumes of each group are shown. Data are quantified as mean ± SEM (n = 6); *p < 0.05 compared with relative control.

Lnc-CCNH-8 overexpressed HCC cells to screen the target genes related to tumor immunity from the differentially expressed gene. As shown in Figures 3A and S7, we found that CD274 (PD-L1) was significantly up-regulated. It is widely reported that PD-L1 was up-regulated in many human cancers and it can interact with PD-1 to inhibit T cell activation, induce apoptosis of effector T cells, and ultimately impair the antitumor immunity.[12] Therefore we hypothesized that PD-L1 mediates the function of Lnc-CCNH-8 in promoting immune escape of HCC. To verify this assumption, the expression of PD-L1 was examined using qPCR (Figure 3B) and western blot (Figure 3C) both in Lnc-CCNH-8 overexpression and Lnc-CCNH-8 knockdown (KD) HCC cells to infer that Lnc-CCNH-8 positively regulated the expression of PD-L1. Consistent results were also demonstrated by flow cytometry analysis of surface PD-L1 expression (Figures 3D and S8). In the subcutaneous tumor tissue sample (Figure 2G), we further detected the expression of PD-L1 in the tumor tissue by immunohistochemical and immunofluorescence (IF) staining. As expected, the expression of PD-L1 was relatively higher in the Lnc-CCNH-8 overexpression group than that in the control group (Figures 3E and 3F). Next, we also tested the expression of PD-L1 and Lnc-CCNH-8 in HCC tissue samples, and the data show that there is a significant positive correlation between PD-L1 and Lnc-CCNH-8 (Figure 3G). Taken together, PD-L1 is a novel downstream target of Lnc-CCNH-8, and its expression is positively regulated by Lnc-CCNH-8.

Lnc-CCNH-8 promotes immune escape of HCC via PD-L1

We then investigated whether modulation of PD-L1 by Lnc-CCNH-8 could affect the immune escape of HCC. The cytotoxicity of $CD8^+$ T cells co-cultured with HCC cells was assessed using LDH cytotoxicity kits. As shown in Figure 4A, overexpression of Lnc-CCNH-8 significantly reduced the proportion of cell apoptosis after incubation with $CD8^+$ T cells at different effector/target (E/T) ratios. Subsequently, the subcutaneous tumor tissue was digested into a single-cell

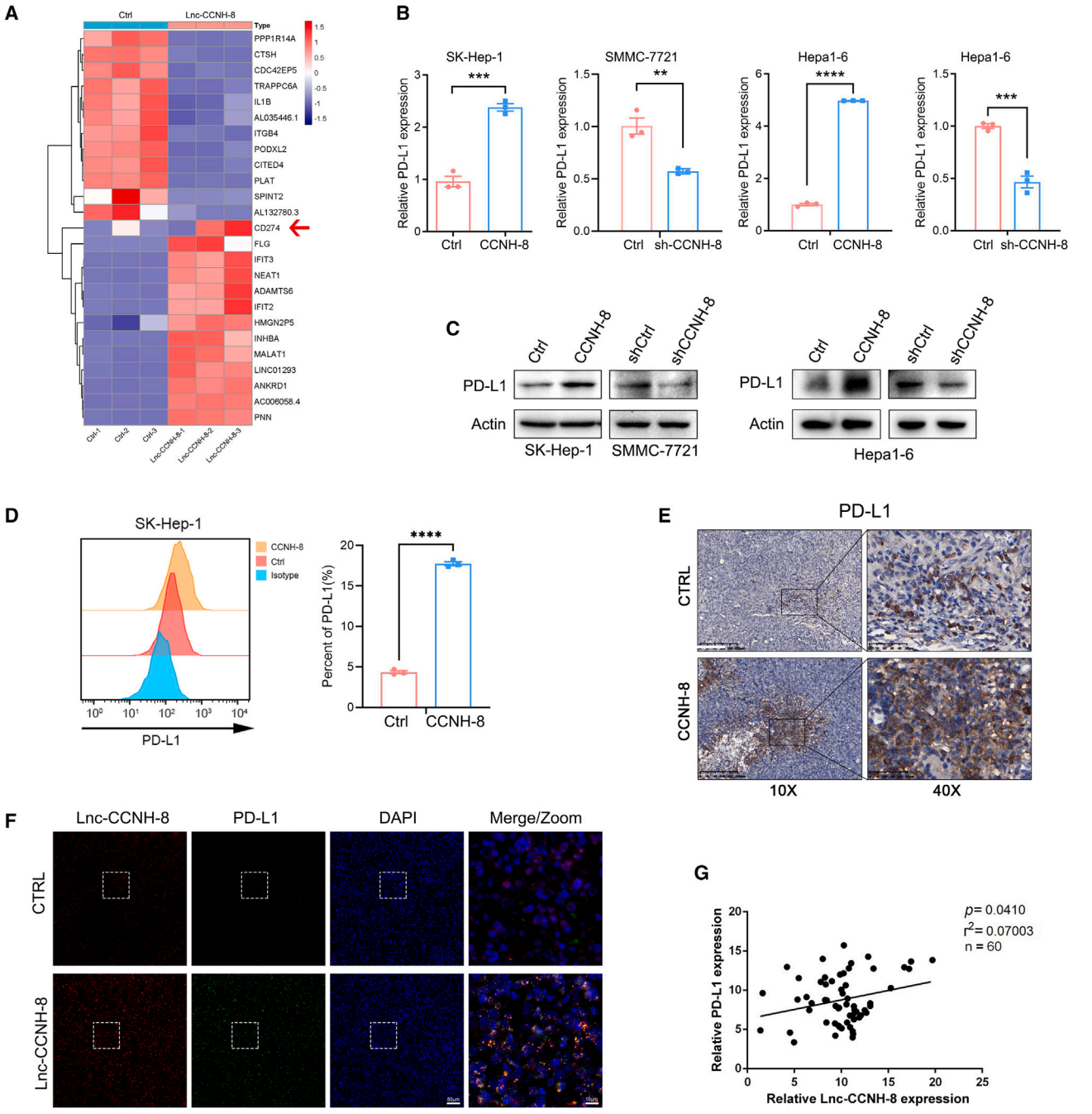

Figure 3. Up-regulation of Lnc-CCNH-8 promotes the expression of PD-L1

(A) Heatmap representation of the differential gene abundance profile in ctrl and Lnc-CCNH-8-overexpressed groups. (B and C) RT-PCR (B) and western blot (C) data showing the expression of PD-L1 in SK-Hep-1, SMMC-7721, and Hepa1-6 cell lines of each group. Data were quantified as mean ± SEM (n = 3). (D) The expression of PD-L1 on SK-Hep-1 cell membrane was detected using flow cytometry after overexpression of Lnc-CCNH-8. (E) Representative images showing the expression level of PD-L1 in subcutaneous tumors of C57BL/6 mice. Magnification: 40×; scale bar: 50 μm. (F) Representative fluorescence images of Lnc-CCNH-8 and PD-L1 in subcutaneous tumors tissue. (G) PD-L1 expression was positively correlated with Lnc-CCNH-8 expression in HCC patients (n = 60). *p < 0.05, **p < 0.01, and ***p < 0.001 compared with relative control.

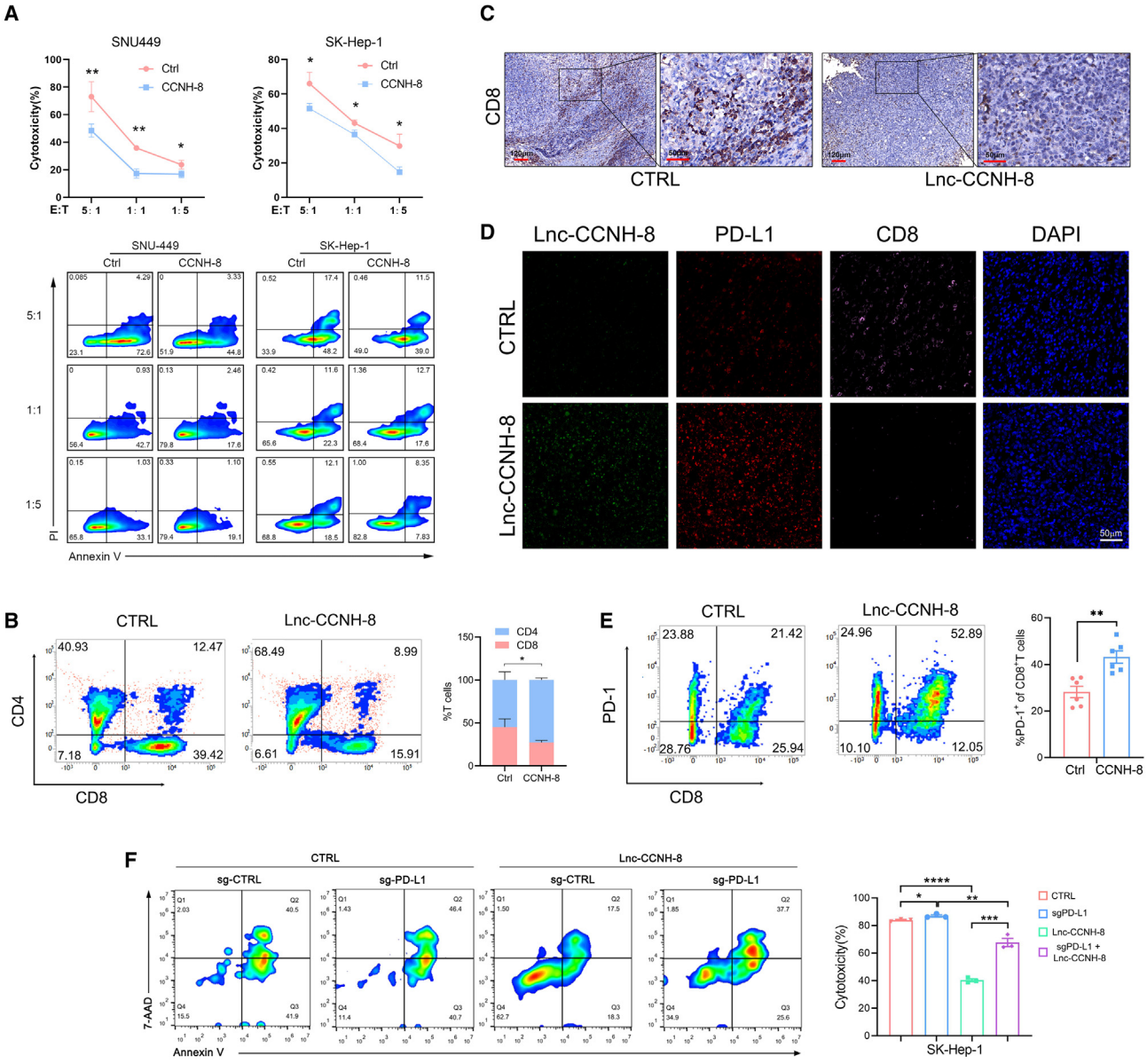

Figure 4. Lnc-CCNH-8 induces tumor immune escape by up-regulating PD-L1 expression

(A) Annexin-V-APC/PI double labeling was used to detect T-cell-mediated apoptosis of SNU-449 and SK-Hep-1 cells. (B and C) Representative images of flow cytometry (B) and immunohistochemical staining (C) of $CD8^+$ T cells in subcutaneous tumor tissue. Magnification: 40×; scale bar: 50 μm. (D) Representative fluorescence images of Lnc-CCNH-8, PD-L1, and CD8 in subcutaneous tumors tissue. (E) Expression levels of PD-1 in tumor tissue infiltrated $CD8^+$T cells were determined using flow cytometry. Data were quantified as mean ± SEM (n = 3). *$p < 0.05$ and **$p < 0.01$ compared with relative control.

suspension and flow cytometry study showed that Lnc-CCNH-8 significantly reduced the tumor infiltrating $CD8^+$ T lymphocytes (Figure 4B). A similar result was found in immunohistochemical and IF staining (Figures 4C and 4D). More important, Lnc-CCNH-8 overexpression also led to a notable increase in PD-L1 expression within the tumor (Figure 4D). In addition, the PD-1 expression of tumor infiltrating $CD8^+$ T cells was significantly increased (Figure 4E), suggesting that Lnc-CCNH-8 may affect the efficacy of checkpoint blockade therapy. To verify that Lnc-CCNH-8 promotes tumor immune escape via PD-L1, we knocked down PD-L1 in SK-Hep-1 cells (Figure S9) and overexpressed Lnc-CCNH-8 simultaneously. The results of the T-cell-mediated tumor cell killing experiment showed that PD-L1 KD significantly weakened the down-regulation of tumor cell killing by T cells induced by Lnc-CCNH-8 (Figure 4F). Therefore,

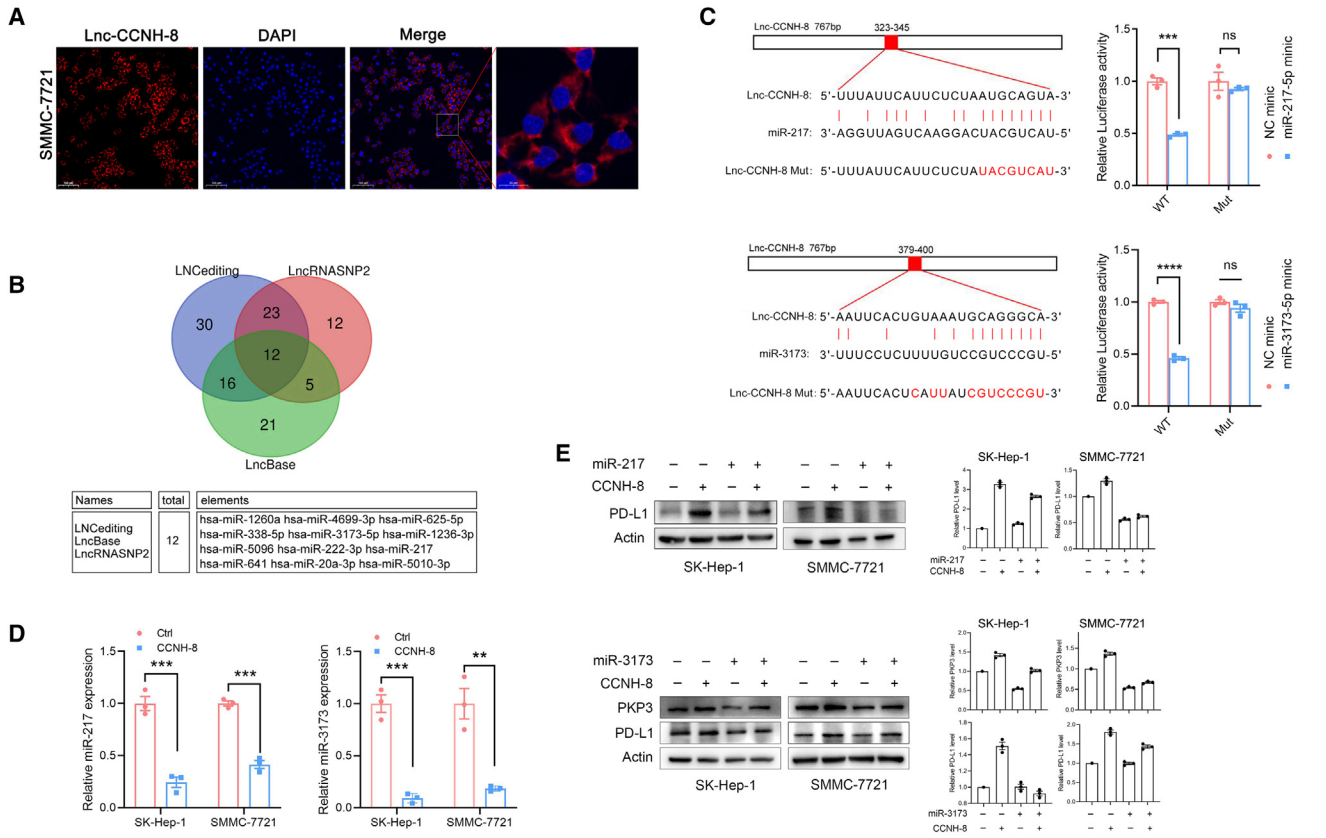

Figure 5. Lnc-CCNH-8 regulates PD-L1 expression through miR-217 and miR-3173

(A) Fluorescence *in situ* hybridization assay used to examine the expression and location of Lnc-CCNH-8 in SMMC-7721. (B) LNCediting, lncRNASNP2, and LncBase were used to predict the targeting microRNA of Lnc-CCNH-8. (C) Lnc-CCNH-8 binding site (top) to miR-217-5p and miR-3173-5p. Luciferase reporter assay (bottom) was performed to detect the interaction between Lnc-CCNH-8 and miRNA. (D) Relative expression levels of miR-217-5p and miR-3173-5p were detected using RT-PCR. (E) PD-L1 and PKP3 expression levels were detected using western blotting. Data are quantified as mean ± SEM (n = 3). *p < 0.05, **p < 0.01, ***p < 0.001 compared with relative control.

Lnc-CCNH-8 promoted tumor immune escape in HCC by up-regulating PD-L1 expression. However, the specific regulatory mechanism of Lnc-CCNH-8 on PD-L1 and the role of Lnc-CCNH-8 in immune checkpoint blockade (ICB) therapy remain to be further investigated.

Lnc-CCNH-8 upregulates PD-L1 expression by acting as a microRNA sponge for miR-217 and miR-3173

To further determine the sub-cellular localization of Lnc-CCNH-8, fluorescence *in situ* hybridization (FISH) analysis was carried out in SMMC-7721 cells, and the results suggested that Lnc-CCNH-8 was located mainly in the cytoplasm (Figure 5A).

It is well known that cytoplasm LncRNAs can act as competing endogenous RNA (ceRNA) to regulate gene expression.[13] We hypothesized that Lnc-CCNH-8 acts as a microRNA (miRNA) sponge to be responsible for PD-L1 up-regulation. We first predicted the target miRNAs of Lnc-CCNH-8 using LNCediting, LncRNASNP2, and LncBase (Figure 5B). We predicted 12 potential target miRNAs and according to the previous studies of these miRNAs, we selected 6 miRNAs (miR-338, miR-3173, miR-222, miR-217, miR-20a, and miR-5010) for further validation. The luciferase reporter assay showed that both miR-3173 and miR-217 could efficiently reduce the luciferase activity of the Lnc-CCNH-8 reporter (Figure S10). Furthermore, both miR-217and miR-3173 failed to reduce the luciferase activity of the Lnc-CCNH-8 reporter when the potential miRNA-binding sites were mutated (Figure 5C). Overexpression of Lnc-CCNH-8 decreased the levels of miR-217 and miR-3173 (Figure 5D). Thus, the above data suggest a role for Lnc-CCNH-8 as a ceRNA in sponging miR-217 and miR-3173. It has been reported that PD-L1 is a direct target of miR-217,[7] whereas miR-3173 was able to target PKP3, which is involved in facilitating the deubiquitination of PD-L1.[14]

We further confirmed that whether miR-217 and miR-3173 were able to decrease PD-L1 or PKP3 expression and whether Lnc-CCNH-8 may rescue the effect of miR-217 and miR-3173. Western blot study shows that miR-217 significantly reduced the protein level of PD-L1, but this effect was rescued by Lnc-CCNH-8 overexpression

(Figure 5E). Second, miR-3173 significantly reduced the protein level of PKP3 and PD-L1, and this effect was also rescued by Lnc-CCNH-8 overexpression (Figure 5E). On the contrary, miR-217 inhibitor further enhanced the up-regulation of Lnc-CCNH-8 on PD-L1 expression (Figure S11). Therefore, the above results show that Lnc-CCNH-8 affects the expression of PD-L1 via sponging both miR-217 and miR-3173.

Lnc-CCNH-8 increases therapeutic sensitivity to anti-PD-L1 treatment

To further investigate the influence of Lnc-CCNH-8 on anti-PD-L1 therapy, we used an anti-PD-L1 mAb to treat C57BL/6 mice inoculated with Hepa1-6 cells overexpressing the control vector or Lnc-CCNH-8 (Figure 6A). Tumor-bearing mice were treated with PD-L1 mAb or PBS. The expression of Lnc-CCNH-8 in the subcutaneous tumor was verified using qPCR (Figure 6D). As shown in Figures 6B, 6C, and 6D, PD-L1 mAb did not significantly inhibit the growth of Hepa1-6 cell tumors in the control group, but PD-L1 mAb significantly inhibited the growth of tumors with Lnc-CCNH-8 overexpression, suggesting that high expression of Lnc-CCNH-8 may improve the sensitivity of tumors to anti-PD-L1 treatment. We also detected $CD8^+$ T cell infiltration, $FoxP3^+$ regulatory T cells (Tregs) and PD-L1 expression in the tumor tissue. Firstly, consistent with the previous results in Figure 4C, Lnc-CCNH-8 significantly impairs the infiltration of $CD8^+$ T cells into the tumor; interestingly, in the anti-PD-L1-treated mouse, overexpression of Lnc-CCNH-8 significantly increases the number of infiltrating $CD8^+$ T cells (Figure 6F). This is also confirmed by flow cytometry analysis (Figure 6G). Second, Lnc-CCNH-8 significantly promoted the expression of PD-L1 in the tumor (Figure 6F), thus showing a better treatment response to the anti-PD-L1 therapy, as indicated by the TUNEL assay in the tumor, showing that the apoptosis of tumor cells was significantly increased in the Lnc-CCNH-8 overexpression group (Figure 6H). Third, significantly higher levels of $FoxP3^+$ Tregs were observed in tumors overexpressing Lnc-CCNH-8, whereas in the anti-PD-L1-treated mouse, overexpression of Lnc-CCNH-8 does not affect $FoxP3^+$ Treg infiltration (Figure 6F). Many studies have described that intratumoral $CD39^+$ $CD8^+$ T cells as tumor-specific and reactive cells[15,16] could predict the response to PD-1 and PD-L1 blockade.[17] Therefore, we further determined the level of $CD39^+$ $CD8^+$ T cells in tumor tissue. As shown in Figure 6G, Lnc-CCNH-8 significantly increased the intratumoral $CD39^+$ $CD8^+$ T cells in the anit-PD-L1 treatment group. This again indicated that Lnc-CCNH-8 enhanced the treatment response of tumors to PD-L1 blockade. Taken together, these results demonstrate that elevated Lnc-CCNH-8 expression increased the therapeutic sensitivity of PD-L1 mAb therapy. High Lnc-CCNH-8 level may be an indicator of therapeutic sensitivity to PD-L1 mAb in HCC.

HBV infection promotes Lnc-CCNH-8 expression via INF-γ/STAT1 signal

To explore the mechanism leading to the up-regulation of Lnc-CCNH-8 in HCC, we hypothesized that the inflammatory microenvironment caused by HBV infection might lead to the up-regulation of Lnc-CCNH-8, as the clinicopathological analysis indicated that higher expression of Lnc-CCNH-8 was significantly associated with higher HBV DNA content. To confirm this speculation, an orthotopic transplantation tumor model of liver cancer was established in C57/BL6 mice and a recombinant adeno-associated virus (AAV) carrying a replicable HBV genome (AAV/HBV) was injected through the tail vein.[18] Immunohistochemical staining of HBsAg in the tumor tissue showed that HBsAg was highly expressed in the tumor of HBV-infected mice compared with the control group (Figure 7A), indicating that the HBV infection model was successfully established. The expression of Lnc-CCNH-8 was detected in the tumor tissue and the data indicated that Lnc-CCNH-8 expression was significantly up-regulated in HBV-infected tumors (Figure 7B). HBV infection can induce the formation of a chronic inflammatory microenvironment, resulting in the up-regulation of a variety of inflammatory factors, including IFN-γ. HBV was also found to significantly upregulate IFN-γ levels in mouse liver tissue in our animal model (Figure 7C). To further explore the mechanism of up-regulation of Lnc-CCNH-8 expression caused by HBV infection, we examined the regulatory effects of IFN-γ on Lnc-CCNH-8 expression in HCC cells, and the results showed that IFN-γ induced the expression of Lnc-CCNH-8 in a dose-dependent manner (Figure 7D). It has been reported that IFN-γ can regulate the expression of downstream target genes through STAT1 signaling pathway.[19] Therefore, STAT1 inhibitor fludarabine was used and it showed significantly inhibition of the IFN-γ-induced up-regulation of Lnc-CCNH-8 expression (Figure 7E). Meanwhile, the expression of PD-L1 is also significantly inhibited by fludarabine (Figure 7F), indicating that IFN-γ promotes the expression of Lnc-CCNH-8 and PD-L1 through STAT1 signaling pathway. STAT1 can bind to gamma-activated sequences (GAS) in the promoter region of target genes, and then regulate their transcription.[19] Therefore, we analyzed the promoter region of Lnc-CCNH-8 and found six potential conserved GAS sequences (Figure 7G). The promoter region of Lnc-CCNH-8 containing these 6 GAS sequences was further cloned into the luciferase reporter vector. The luciferase activity assay showed that IFN-γ could significantly up-regulate the activity of the reporter (Figure 7H), indicating that IFN-γ indeed up-regulated the transcription of Lnc-CCNH-8 by regulating the binding of STAT1 to the promoter region of Lnc-CCNH-8.

Lnc-CCNH-8 as a potential predictive marker for immunotherapy response in HCC

The above data have confirmed that Lnc-CCNH-8 promotes immune escape of HCC via regulation of PD-L1 expression. To further explore whether Lnc-CCNH-8 can act as a potential biomarker for predicting immunotherapy efficacy, we first ask whether the expression of Lnc-CCNH-8 can be detected in the plasma of HCC patients. Circulating exosomal non-coding RNAs can be used as markers for the diagnosis and prognosis of liver cancer.[20] We first extracted plasma exosomes from HCC patients and healthy volunteers, then the electron microscopy, particle size analysis and western blot analysis of exosome marker proteins confirmed the presence of exosomes in plasma samples (Figures 8A–8C). qPCR analysis showed that Lnc-CCNH-8 could be detected in plasma exosomes. More important, the expression of Lnc-CCNH-8 was significantly higher in the plasma exosomes

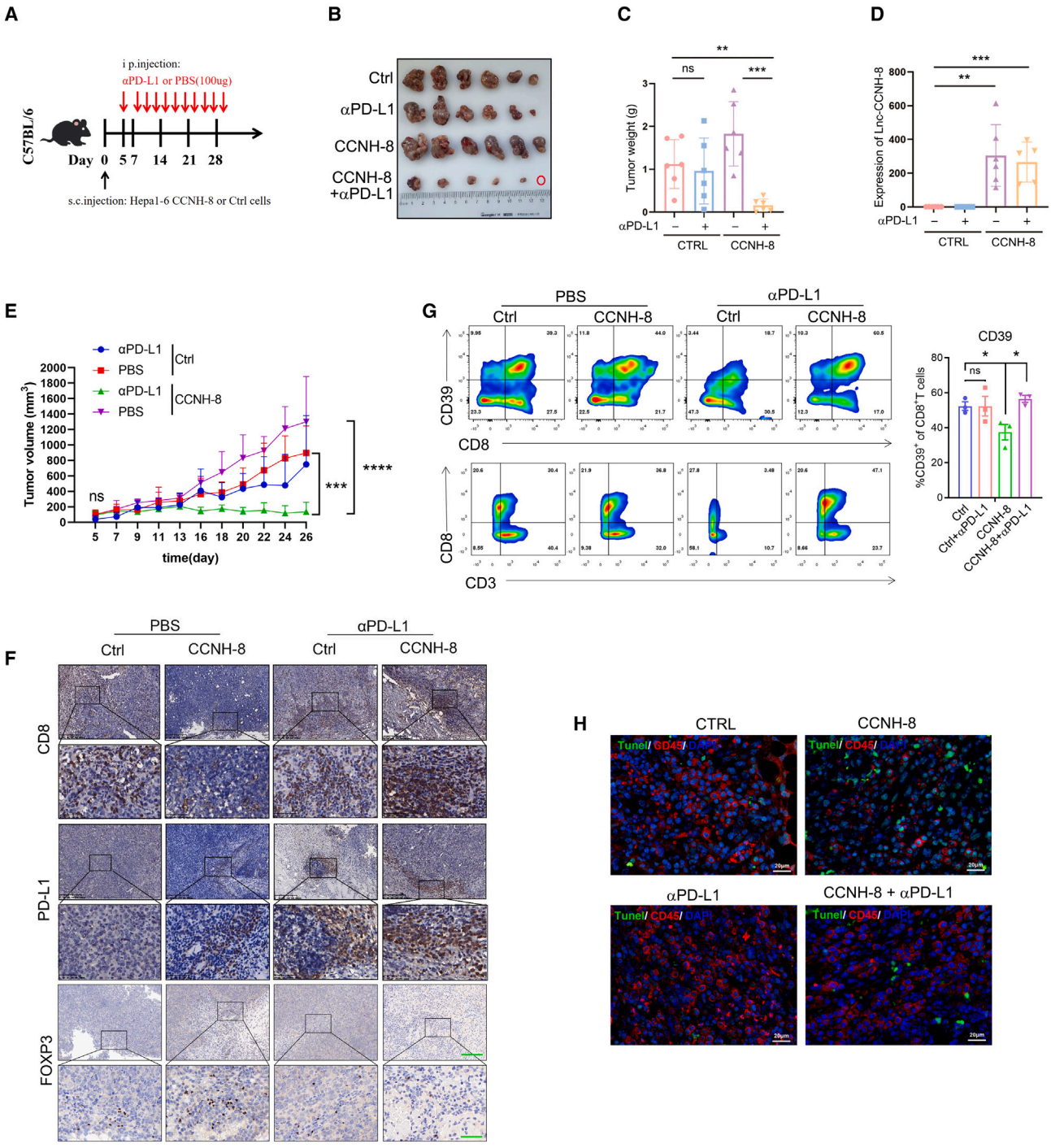

Figure 6. Lnc-CCNH-8 enhances therapeutic sensitivity to anti-PD-L1 treatment

(A) Therapeutic model of subcutaneous tumor in C57BL/6 mice. Hepa1-6 cells were transfected with ctrl or Lnc-CCNH-8 and injected into the C57BL/6 mice. The mice were treated with PBS or anti-PD-L1. (B) Images of xenografts in mice from each group. (C and D) Quantification of tumor weight (C) in mice of each group after 24 days of injection. The expression level of Lnc-CCNH-8 (D) in each group was detected using RT-PCR. Data were quantified as mean ± SEM (n = 6). (E) Growth curve of tumor formation in mice of each group. Data are mean ± SEM (n = 6). (F) Immunohistochemical staining showed the expression levels of CD8, PD-L1, and FoxP3 in each group. (G) Expression levels of $CD39^{+}CD8^{+}$ T cells in tumor tissues were detected using flow cytometry. (H) Representative fluorescence images of TUNEL (green) and $CD45^{+}$ (red) in each group. Red fluorescence represents $CD45^{+}$ T cells. Green fluorescence represents apoptotic cells. Scale bar: 20 μm. $^{**}p < 0.01$ and $^{***}p < 0.001$ compared with relative control.

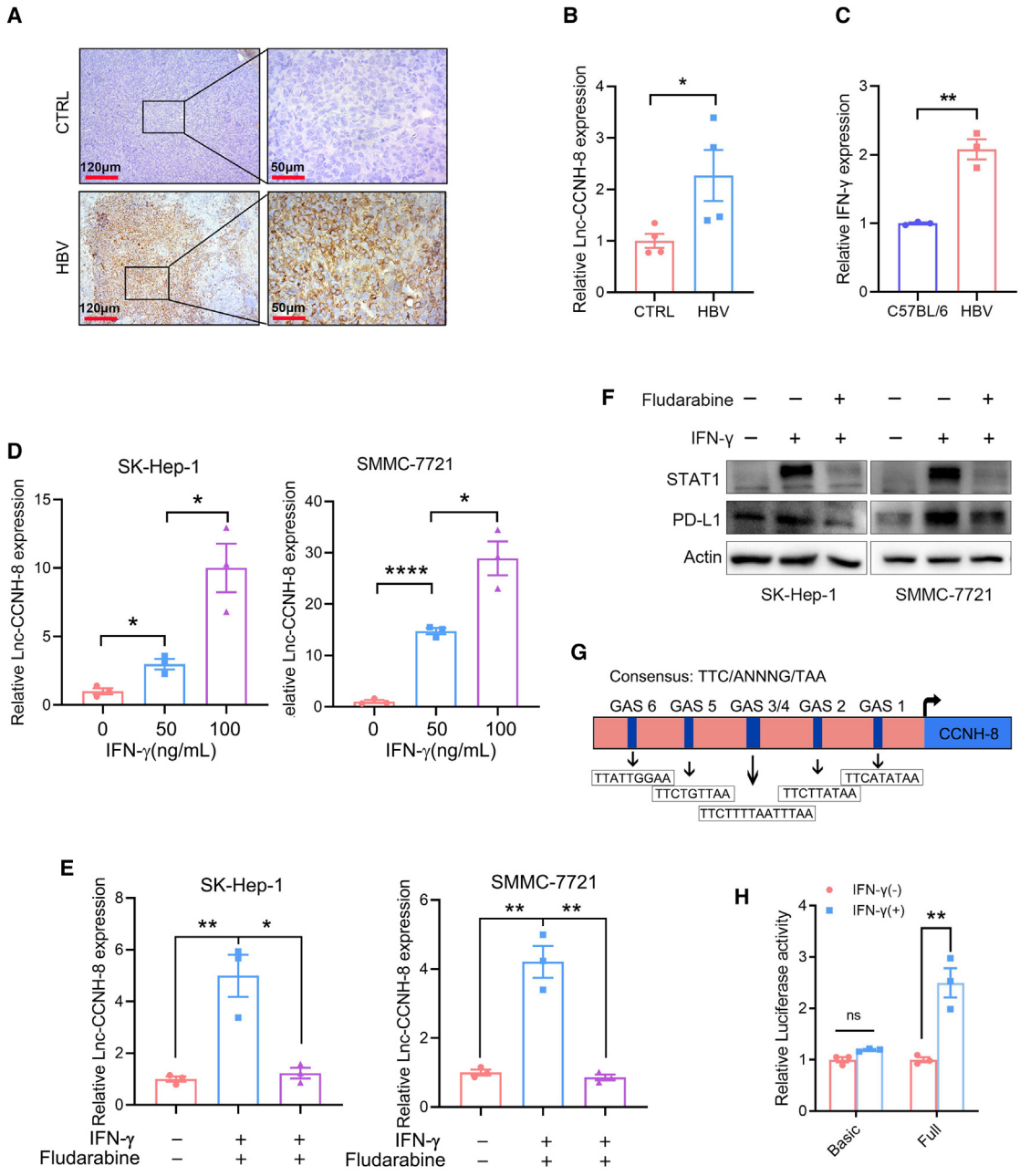

Figure 7. HBV infection promotes Lnc-CCNH-8 expression via INF-γ/STAT1 signaling

(A) Representative images showing the HBV levels (detected by IHC) in orthotopic tumors of C57BL/6 mice. Magnification: 40×; scale bar: 50 μm. (B) Expression of Lnc-CCNH-8 in orthotopic tumors was detected using RT-PCR. (C) The expression of IFN-γ in the liver tissue of the mice was determined by ELISA. (D) RT-PCR performed on the SK-Hep-1 and SMMC-7721 cells treated with IFN-γ (100 ng/mL). (E) RT-PCR showed the expression of Lnc-CCNH-8 in SK-Hep-1 and SMMC-7721 cells after treatment with fludarabine (1 μM) and IFN-γ (100 ng/mL). (F) Western blotting performed on the SK-Hep-1 and SMMC-7721 cells 24 h after treatment with fludarabine (1 μM) or IFN-γ (100 ng/mL) against STAT1 and PD-L1. (G) The predicted STAT1 binding site on the Lnc-CCNH-8 promoter was obtained from JASPAR. GAS, gamma-activated sequence. (H) The luciferase activity assay performed on the 293T cells with or without treatment with IFN-γ (100 ng/mL). Data are quantified as mean ± SEM (n = 3). *p < 0.05, **p < 0.01, and ***p < 0.001 compared with relative control.

of HCC patients compared with the sample of healthy volunteers (Figure 8D), which was consistent with the results detected in tumor tissues. We further detected the expression of Lnc-CCNH-8 in HCC patients treated with immunotherapy (including anti-PD-1 and anti-PD-L1 therapy), and evaluated the relationship between the expression of Lnc-CCNH-8 and the efficacy of immunotherapy. The results

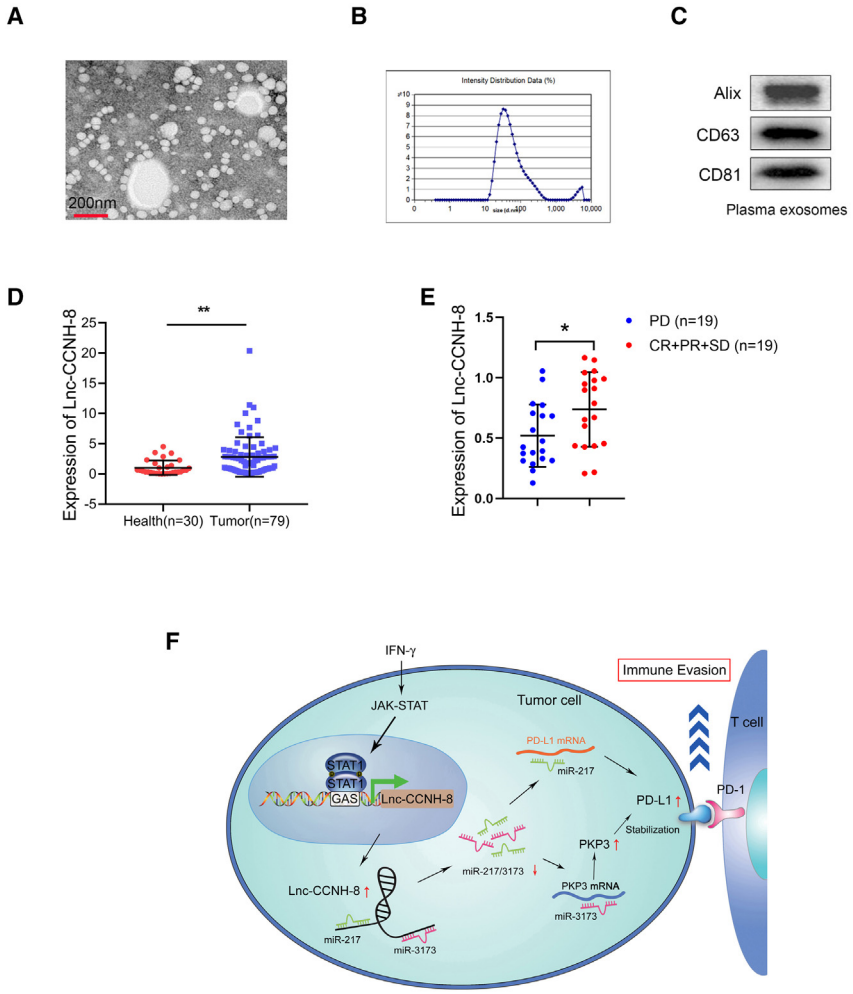

Figure 8. Lnc-CCNH-8 as a potential predictive marker for immunotherapy response in HCC

(A) Morphology of exosomes by electron microscopy. Scale bar: 200 nm. (B) Particle size analysis of exosomes. (C) Exosome marker proteins Alix, CD63, and CD81 were detected using western blot. (D) Expression level of Lnc-CCNH-8 (detected using RT-PCR) in plasma-derived exosomes from HCC patients (n = 79) and healthy individuals (n = 30). **p < 0.01. (E) Expression level of Lnc-CCNH-8 (detected using RT-PCR) under therapeutic efficacy. PD, progressive disease; CR, complete response; PR, partial response; SD, stable disease. *p < 0.05. (F) Schematic diagram: Lnc-CCNH-8 promotes immune escape by up-regulating PD-L1 via dual mechanisms in hepatocellular carcinoma.

showed that Lnc-CCNH-8 expression was relatively low in patients with progressive disease (PD) after immunotherapy (n = 19), while in the group of patients with better immunotherapy outcomes (including complete response [CR], partial response [PR], and stable disease [SD]; n = 19), Lnc-CCNH-8 expression was higher, indicating that patients with high Lnc-CCNH-8 expression responded better to anti-PD-1 and anti-PD-L1 therapy (Figure 8E). Taken together, these results demonstrate that Lnc-CCNH-8 may serve as a predictive marker for immunotherapy response in HCC.

DISCUSSION

LncRNAs have been identified to function as key regulators of physiological and pathological processes including cancer initiation and progression. However, the role of lncRNAs in tumor immune escape remains poorly understood. In this study, we first screened for aberrantly expressed lncRNAs in HCC tissues by transcriptome sequencing and found that Lnc-CCNH-8 was overexpressed in HCC tissues. Subsequent clinicopathological correlation analysis showed that Lnc-CCNH-8 expression was associated with poor prognosis, tumor size, AFP, and HBV DNA in patients with HCC. Therefore, the present study aims to demonstrate the possible mechanism by which Lnc-CCNH-8 is involved in HCC development. Taken together, Lnc-CCNH-8 acts as ceRNAs of miR-217 and miR-3173, and then up-regulates PD-L1 expression, so as to suppress T cell activity, and ultimately accelerates the immune escape of HCC cells. More important, Lnc-CCNH-8 overexpressing HCC exhibited remarkable therapeutic sensitivity to PD-L1 mAb treatment in a mouse model. We characterized a regulatory mechanism of lncRNA-mediated immune escape in HCC and highlighted that Lnc-CCNH-8 could act as a potential therapeutic target to enhance the efficacy of PD-1/PD-L1 antibodies.

Up-regulation of PD-L1 expression is one of the important mechanisms of immune escape of tumor cells. PD-L1 has been shown to be regulated at the transcriptional, post-transcriptional, and post-translational levels.[12] A variety of cytokines and exosomes in the tumor microenvironment can induce PD-L1 expression. IFN-γ is the most prominent stimulator contributing to the inducible expression of PD-L1 [2]. IFN-γ has multiple ways to induce PD-L1 expression, depending on the type of tumor, including the JAK2/STAT1/IFR-1 signaling pathway in gastric cancer[21] and the JAK/STAT3 and PI3K-AKT signaling pathways in lung cancer.[22] Cancer-derived miRNAs are important post-transcriptional regulators of PD-L1 expression in the TME. CD274 mRNA was the direct target of multiple oncogenic miRNAs such as miR-34a, miR-200 family, miR-142-5p, miR-424, miR-214, miR-497-5p, and miR-140.[12] In this study, we show that Lnc-CCNH-8 sponges both miR-217 and miR-3173. miR-217 can directly target PD-L1 mRNA, while miR-3173 targets PKP3, which stabilizes PD-L1 via the post-translational level. Finally, Lnc-CCNH-8 regulates the expression of PD-L1 by sponging both miR-217 and miR-3173. Thus, our data reveal a novel mechanism that regulates PD-L1 expression.

Only a fraction of HCC patients respond to ICB treatment. Inflamed and non-inflamed classes of HCC and genomic signatures have been

associated with response to ICIs, but no validated biomarker is available to guide clinical decision making. In contrast to lung and urothelial cancers, evidence for a predictive role of PD-L1 immunostaining in HCC is lacking.[23] Therefore, there is an urgent need to find indicators to predict the efficacy of immunotherapy in HCC. Recently, exosomal ncRNAs have emerged as novel players in the initiation and development of various human diseases, including cancer.[24] Exosomal ncRNAs exert potential to be candidate biomarkers and therapeutic targets for cancer. Recent research has focused on exosomes as potential biomarkers because they can be detected in many body fluids using simple and inexpensive methods. Zhang et al.[25] found that higher serum exosomal lncRNA SBF2-AS1 levels from recurrent glioblastoma patients were associated with worse prognosis and poorer response to temozolomide treatment, suggesting that human serum exosomal lncSBF2-AS1 can serve as a potential diagnostic marker for therapy-resistant glioblastoma. In our study, plasma exosomal Lnc-CCNH-8 levels from HCC patients were associated with response to anti-PD-1 and anti-PD-L1 therapy, suggesting that exosomal Lnc-CCNH-8 can serve as a predictive marker for immunotherapy response in HCC.

HBV infection is still one of the most dangerous viral diseases. Many individuals with hepatitis B eventually develop HCC. Compared with non-virus-related HCC, the level of PD-L1 was significantly higher in HBV-related HCC.[26] To some extent, the innate immune and inflammatory responses of the host dominate HBV infection and liver pathogenesis. The inflammatory cytokines induced by HBV infection may up-regulate the expression of PD-L1 at the transcriptional level through the classical JAK/STAT signaling pathway. In addition, studies have shown that HBV can increase PD-L1 expression through the PTEN/β-catenin/c-Myc signaling pathway.[27] However, it still remains largely unknown as to how HBV infection elevates PD-L1 expression in hepatocytes. Our study proposes that Lnc-CCNH-8 mediates HBV-induced up-regulation of PD-L1. Specifically, HBV infection activates the JAK/STAT signaling pathway through inflammatory cytokine INF-γ, promotes the binding of STAT1 to the GAS sequence of the Lnc-CCNH-8 promoter region, and up-regulates the transcription of Lnc-CCNH-8. And Lnc-CCNH-8 up-regulates the expression of PD-L1 through the miR-217 and miR-3173/PKP3 pathways, and finally promotes immune escape of HCC. Our study provides a novel explanation for the up-regulation of PD-L1 caused by HBV.

MATERIALS AND METHODS

Human specimens

HCC and paired adjacent normal liver tissues were obtained after surgery from the bio-bank of Mengchao Hepatobiliary Hospital of Fujian Medical University. All the enrolled patients were diagnosed with HCC and had received no relevant treatment prior to surgery. Sample collection and use were approved by Mengchao Hepatobiliary Hospital Medical Ethics Committee of Fujian Medical University (2021_053_01). Meanwhile, informed consent was provided by the patients.

Cell culture and reagents

Human HCC cell lines SK-Hep-1, HepG2, and Hep3B and human embryonic kidney cell line HEK293T were obtained from American Type Culture Collection (ATCC). SMMC-7721 was obtained from Second Military Medical University. Human HCC cell lines QGY-7701 and BEL-7401 and mouse liver cancer cell line Hepa1-6 were purchased from the Chinese Academy of Science (Shanghai, China). SK-Hep-1, SMMC-7721, Hepa1-6, QGY-7701, and BEL-7401 were cultured with DMEM (Gibco). Hep3B and HepG2 were cultured in MEM (Gibco). All mediums were supplemented with 10% fetal bovine serum (FBS), 100 IU/mL penicillin, and 100 mg/mL streptomycin (Gibco). Fludarabine was purchased from Selleck.

Cell transfection

Specific short hairpin RNA (shRNA) against Lnc-CCNH-8 (shCCNH-8) and sh-NC were synthesized by Sangon Biotech. pCDH-CMV-EF1-CopGFP-T2A-puro vector targeting Lnc-CCNH-8 and empty vector were constructed by our laboratory. To construct stably modified cell lines, overexpression plasmids pCDH-CMV-CCNH-8-EF1-CopGFP-T2A-puro, KD plasmids pLKO.1-shCCNH-8, and their respective empty plasmids were applied to generated lentivirus. When the cells grew to approximately 40–50% density in 6-well plates, 2 mL of fresh media supplemented with 1 μL of polybrene (MCE) and 100 μL lentivirus was added. Infected cell lines were further selected by 2 μg/mL puromycin (MCE) and verified using qRT-PCR.

Luciferase reporter assay

The pmiRGLO dual-luciferase vector containing Lnc-CCNH-8 sequence was co-transfected with miR-217-5p or miR-3173-5p into 293T cells. After 36 h, luciferase reporter assays were performed using the TransDetect Double-Luciferase Reporter Assay Kit (TransGen Biotech).

Animal studies

The B-NDG (NOD.CB17-Prkdcscid Il2rgtm1/Bcgen) mice (female, 4 weeks) were purchased from Biocytogen. C57BL/6 mice (male, 6–8 weeks) were purchased from China Wushi, Inc. (Shanghai, China). All mice were maintained under specific pathogen-free conditions. All animal experiments were approved by the Animal Ethics Committee of Mengchao Hepatobiliary Hospital of Fujian Medical University.

Tumor xenograft model

For subcutaneous tumor model, B-NDG and C57BL/6 mice were injected into the right underarm with Matrigel (Corning) containing transfected Lnc-CCNH-8 or empty SK-Hep-1 or hepa1-6 cells (3×10^6 cells) (1:1). Tumor volume was calculated every 2 days. Mice were sacrificed when the tumor size reached 2,000 mm^3. Tumor tissues were then harvested for RNA extraction, and Lnc-CCNH-8 expression was detected using qRT-PCR. Additional tumor tissues were used for immunohistochemistry and flow cytometry. To verify the curative effect of point-blocking therapy by Lnc-CCNH-8, the treatment was started when the tumor size reached 50 mm^3. Mice were injected intraperitoneally every 3 days and treated with

αPD-L1 (BE0101 [BioXcell], 100 μg/mouse) or PBS solution (as control), until day 28.

RNA sequencing

HCC tumor tissue and adjacent non-tumor tissue from 61 patients were used for RNA sequencing (RNA-seq) analysis. Sequencing libraries were prepared using the VAHTS Universal V6 RNA-seq Library Prep Kit from Illumina (Vazyme,) according to the manufacturer's instructions. Whole transcriptome sequencing (paired end, 150 bp) was performed on the libraries using Illumina HiSeq X10 at Annoroad Gene Technology Co., Ltd. (Beijing, China). The Illumina short reads were aligned to the human reference genome (Ensembl GRCh38) with annotations (GENCODE GRCh38 version 32) using STAR (version 2.6.0) in 2-pass mode, followed by quantification of annotated transcripts using RSEM (version 1.3.1). Differential expression analysis was performed using R software. Genes with $|\log_2(\text{fold change})| > 1$ and false discovery rate (FDR) < 0.05 were considered to be differentially expressed in HCC tissues and matched para-tumor tissues.

Real-time qPCR

Total RNA extraction was isolated from fresh-frozen tissues and cell lines using the TransZol Up Plus RNA Kit (TransGen Biotech). Synthesis of cDNA was performed using the Transcriptor First Strand cDNA Synthesis Kit (Roche, Basel, Switzerland). Relative expression levels were detected using real-time qPCR with SYBR Green qPCR Master Mix (DBI; Ludwigshafen, Germany) and an ABI7500 Real-Time PCR instrument. The relative expression of RNA was calculated using the $2^{-\Delta\Delta Ct}$ method. The primer sequences of target genes are shown in Table S2. Human 18S rRNA was used for normalization.

CCK-8 and colony formation assays

Transfected cells were seeded in 96-well plates (2×10^4 cells/well) and incubated for 12, 24, 48, 72, and 96 h. The cells were washed with PBS, and100 μL 10% CCK-8 solution (TransGen Biotech) was added. Optical density was measured at 450 nm after incubation for 2 h.

For colony formation assay, stable transfected cells (5×10^2 cells/well) seeded in 6-well plates were incubated for 7–10 days. The cells were washed twice with PBS, fixed with 4% paraformaldehyde (PFA) for 20 min at room temperature, and stained with crystal violet for 30 min. The plates were then dried for photography. The number of colonies containing more than 50 cells was recorded and analyzed using ImageJ software.

Western blotting

Proteins were extracted using RIPA buffer (Beyotime) supplemented with 1% protease inhibitor cocktails (Roche), and the concentration was measured using BCA Protein Assay Kit (Transgene). The proteins were loaded and run on 10% SDS-PAGE (Bio-Rad), followed by transfer to NC membranes (PALL Corporation). After blocking in 5% BSA for 1 h at room temperature, the membranes were incubated with primary antibodies overnight at 4°C. Then, the membranes were incubated with horseradish peroxidase (HRP)-conjugated secondary antibodies (Abcam) for 1 h at room temperature. The blot signals were visualized using ECL reagent (Pierce) and detected using the ChemiDoc MP Imaging System (Bio-Rad).

The primary antibodies were as follows: β-actin (ab115777; Abcam), PD-L1 (ab205921; Abcam), CD63 (ab134045; Abcam), STAT1 (14994; Cell Signaling Technology), Alix (3A9[2171S]; Cell Signaling Technology), CD81 (cs166029; Santa Cruz), and plakophilin 3 (PKP3) (ab109441; Abcam).

Immunohistochemical staining

Paraffin-embedded tumor tissues were cut into 5 μm slices and dried at 60°C for 2 h. Immunohistochemical staining was performed using the EliVision plus kit (MXB Biotechnologies). The following primary antibodies were used for staining: PD-L1 (64988; Cell Signaling Technology), CD8 (ab217344; Abcam), and HBsAg (MAB-0847; Fuzhou Maixin Biotech Co., Ltd.).

Flow cytometry

Activated T cells were co-cultured with SNU-449 or SK-Hep-1 at different E/T ratios for 24 h. The apoptosis percentage of SNU-449 and SK-Hep-1 cells was detected using flow cytometry using Annexin V-APC/PI Apoptosis Kit (KeyGEN BioTECH) according to the manufacturer's instructions.

For flow cytometry, cells were washed in PBS and centrifuged at an appropriate speed. The cells were then fixed with 4% PFA, washed twice, and blocked with 5% BSA in PBS. After centrifugation, the cells were incubated in the primary antibodies for 30 min. The cells were then washed again and analyzed using flow cytometry (Becton Dickinson). For each independent sample, a total of 10,000 cells were collected for analysis.

The primary antibodies were as follows: GzmB-PE (372208; BioLegend), PD-L1-APC (17-5938-42; Invitrogen), perforin-APC (308112; BioLegend), CD62L-PC5.5 (45-0621-82; eBioscience), CD8-PE (12-0084-82; eBioscience), PD-1-PECy7 (25-9985-82; eBioscience), CD4-FITC (11-0041-82; eBioscience), CD3-APC (17-0031-82; eBioscience), CD8-Pecp-cy5.5 (45-0088-42; eBioscience), and CD44-PECy7 (25-0441-82; eBioscience).

IF

Paraffin-embedded sections of mouse tumor tissue were baked, deparaffinized, and rehydrated, followed by antigen retrieval by treatment with 1× EDTA at 98°C for 10 min. The samples were then washed and permeabilized with 0.2% Triton X-100 (Adamas-beta). After blocking in 5% BSA (in PBS), sections were incubated with primary antibody against CD45 (GB11066; Servicebio) overnight at 4°C, followed by secondary antibody (anti-rabbit Cy3; GB21303; Servicebio). Cell nuclei were counterstained with DAPI (G1012, Servicebio). For TUNEL staining, paraffin sections were stained according to the instructions (FITC Tunel Cell Apoptosis Detection Kit; G1501; Servicebio). Images were captured by fluorescence microscopy.

Exosome isolation and identification

Peripheral blood (5 mL) was collected separately from healthy volunteers and HCC patients. Plasma was isolated from peripheral blood by centrifugation at 3,000 × *g* for 10 min, and 2.5 mL plasma was prepared for exosome isolation. All centrifugation processes were performed at 4°C. First, the plasma was centrifuged at 2,000 × *g* for 30 min. The supernatant was collected and centrifuged again at 10,000 × *g* for 45 min to remove debris and microvesicles. The supernatant was filtered through a 0.22 μm membrane followed by ultracentrifugation at 110,000 × *g* for 2 h (Optima XPN-100; Beckman Coulter). The exosome pellet was washed in 1 mL PBS and resuspended in PBS, followed by an additional step of ultracentrifugation at 110,000 × *g* for 70 min.

The exosome was suspended in PBS and divided into two parts; one was used for the electron microscopy experiment (Servicebio) and the other was analyzed for particle size using a particle size analyzer (Malvern Zetasizer Nano-ZS 300).

Statistical analysis

SPSS Statistics version 25.0 (SPSS, Inc.) and Prism version 8.21 (GraphPad Software) were used for statistical analysis and graphing of qPCR results. Data are presented as mean ± SEM. Paired t tests were used to compare differences between cancer and paracancer, and one-way ANOVA was used to compare three or more groups. Kaplan-Meier curves with log rank tests were used for survival analysis. Univariate and multivariate Cox regression models were used to analyze the independent risk factors for HCC patients. p values <0.05 were considered to indicate statistical significance. All analyses were performed in triplicate.

DATA AND CODE AVAILABILITY

The data used for supporting the findings of this study are available from the corresponding authors upon request.

SUPPLEMENTAL INFORMATION

Supplemental information can be found online at https://doi.org/10.1016/j.omtn.2024.102125.

ACKNOWLEDGMENTS

This work was supported by Science and Technology Projects of Fujian Province (grants 2019Y9047, 2021Y9032, 2022L3030, 2020J011164, and 2021J011291), the Fujian Provincial Health Technology Project (grants 2021ZQNZD014, 2020GGA072, 2021QNA063, and 2020QNA072), the Scientific Foundation of Fuzhou Municipal Health Commission (grants 2021-S-wt2, 2021-S-wt3, 2021-S-wp1, and 2021-S-wq21), and the Scientific Foundation of Fuzhou City (grant 2021-S-100).

AUTHOR CONTRIBUTIONS

B.Z., Yingchao Wang, and X.L. conceptualized the study; B.Z., Yang Wang, X.Z., N.C, Yue Zhong, Yang Zhao, J.H., and X.Q. performed experiments; B.Z., F.W., X.Z., Q.Z., Yingchao Wang, and X.L. performed analysis; B.Z. and X.L. prepared the manuscript.

DECLARATION OF INTERESTS

The authors declare no competing interests.

REFERENCES

1. Sung, H., Ferlay, J., Siegel, R.L., Laversanne, M., Soerjomataram, I., Jemal, A., and Bray, F. (2021). Global Cancer Statistics 2020: GLOBOCAN Estimates of Incidence and Mortality Worldwide for 36 Cancers in 185 Countries. CA A Cancer J. Clin. *71*, 209–249. https://doi.org/10.3322/caac.21660.

2. Zerdes, I., Matikas, A., Bergh, J., Rassidakis, G.Z., and Foukakis, T. (2018). Genetic, transcriptional and post-translational regulation of the programmed death protein ligand 1 in cancer: biology and clinical correlations. Oncogene *37*, 4639–4661. https://doi.org/10.1038/s41388-018-0303-3.

3. Gong, A.Y., Zhou, R., Hu, G., Li, X., Splinter, P.L., O'Hara, S.P., LaRusso, N.F., Soukup, G.A., Dong, H., and Chen, X.M. (2009). MicroRNA-513 regulates B7-H1 translation and is involved in IFN-gamma-induced B7-H1 expression in cholangiocytes. J. Immunol. *182*, 1325–1333. https://doi.org/10.4049/jimmunol.182.3.1325.

4. Wang, W., Li, F., Mao, Y., Zhou, H., Sun, J., Li, R., Liu, C., Chen, W., Hua, D., and Zhang, X. (2013). A miR-570 binding site polymorphism in the B7-H1 gene is associated with the risk of gastric adenocarcinoma. Hum. Genet. *132*, 641–648. https://doi.org/10.1007/s00439-013-1275-6.

5. Wang, X., Li, J., Dong, K., Lin, F., Long, M., Ouyang, Y., Wei, J., Chen, X., Weng, Y., He, T., and Zhang, H. (2015). Tumor suppressor miR-34a targets PD-L1 and functions as a potential immunotherapeutic target in acute myeloid leukemia. Cell. Signal. *27*, 443–452. https://doi.org/10.1016/j.cellsig.2014.12.003.

6. Chen, L., Gibbons, D.L., Goswami, S., Cortez, M.A., Ahn, Y.H., Byers, L.A., Zhang, X., Yi, X., Dwyer, D., Lin, W., et al. (2014). Metastasis is regulated via microRNA-200/ZEB1 axis control of tumour cell PD-L1 expression and intratumoral immunosuppression. Nat. Commun. *5*, 5241. https://doi.org/10.1038/ncomms6241.

7. Miao, S., Mao, X., Zhao, S., Song, K., Xiang, C., Lv, Y., Jiang, H., Wang, L., Li, B., Yang, X., et al. (2017). miR-217 inhibits laryngeal cancer metastasis by repressing AEG-1 and PD-L1 expression. Oncotarget *8*, 62143–62153. https://doi.org/10.18632/oncotarget.19121.

8. Wang, C.J., Zhu, C.C., Xu, J., Wang, M., Zhao, W.Y., Liu, Q., Zhao, G., and Zhang, Z.Z. (2019). The lncRNA UCA1 promotes proliferation, migration, immune escape and inhibits apoptosis in gastric cancer by sponging anti-tumor miRNAs. Mol. Cancer *18*, 115. https://doi.org/10.1186/s12943-019-1032-0.

9. Finn, R.S., Qin, S., Ikeda, M., Galle, P.R., Ducreux, M., Kim, T.Y., Kudo, M., Breder, V., Merle, P., Kaseb, A.O., et al. (2020). Atezolizumab plus Bevacizumab in Unresectable Hepatocellular Carcinoma. N. Engl. J. Med. *382*, 1894–1905. https://doi.org/10.1056/NEJMoa1915745.

10. Finn, R.S., Ikeda, M., Zhu, A.X., Sung, M.W., Baron, A.D., Kudo, M., Okusaka, T., Kobayashi, M., Kumada, H., Kaneko, S., et al. (2020). Phase Ib Study of Lenvatinib Plus Pembrolizumab in Patients With Unresectable Hepatocellular Carcinoma. J. Clin. Oncol. *38*, 2960–2970. https://doi.org/10.1200/JCO.20.00808.

11. Yi, M., Jiao, D., Xu, H., Liu, Q., Zhao, W., Han, X., and Wu, K. (2018). Biomarkers for predicting efficacy of PD-1/PD-L1 inhibitors. Mol. Cancer *17*, 129. https://doi.org/10.1186/s12943-018-0864-3.

12. Yi, M., Niu, M., Xu, L., Luo, S., and Wu, K. (2021). Regulation of PD-L1 expression in the tumor microenvironment. J. Hematol. Oncol. *14*, 10. https://doi.org/10.1186/s13045-020-01027-5.

13. Bach, D.H., and Lee, S.K. (2018). Long noncoding RNAs in cancer cells. Cancer Lett. *419*, 152–166. https://doi.org/10.1016/j.canlet.2018.01.053.

14. Liu, Z., Wang, T., She, Y., Wu, K., Gu, S., Li, L., Dong, C., Chen, C., and Zhou, Y. (2021). N(6)-methyladenosine-modified circIGF2BP3 inhibits CD8(+) T-cell responses to facilitate tumor immune evasion by promoting the deubiquitination of PD-L1 in non-small cell lung cancer. Mol. Cancer *20*, 105. https://doi.org/10.1186/s12943-021-01398-4.

15. Yost, K.E., Satpathy, A.T., Wells, D.K., Qi, Y., Wang, C., Kageyama, R., McNamara, K.L., Granja, J.M., Sarin, K.Y., Brown, R.A., et al. (2019). Clonal replacement of tumor-specific T cells following PD-1 blockade. Nat. Med. *25*, 1251–1259. https://doi.org/10.1038/s41591-019-0522-3.

16. Duhen, T., Duhen, R., Montler, R., Moses, J., Moudgil, T., de Miranda, N.F., Goodall, C.P., Blair, T.C., Fox, B.A., McDermott, J.E., et al. (2018). Co-expression of CD39 and CD103 identifies tumor-reactive CD8 T cells in human solid tumors. Nat. Commun. *9*, 2724. https://doi.org/10.1038/s41467-018-05072-0.

17. Yeong, J., Suteja, L., Simoni, Y., Lau, K.W., Tan, A.C., Li, H.H., Lim, S., Loh, J.H., Wee, F.Y.T., Nerurkar, S.N., et al. (2021). Intratumoral CD39(+)CD8(+) T Cells Predict Response to Programmed Cell Death Protein-1 or Programmed Death Ligand-1 Blockade in Patients With NSCLC. J. Thorac. Oncol. *16*, 1349–1358. https://doi.org/10.1016/j.jtho.2021.04.016.

18. Yang, D., Liu, L., Zhu, D., Peng, H., Su, L., Fu, Y.X., and Zhang, L. (2014). A mouse model for HBV immunotolerance and immunotherapy. Cell. Mol. Immunol. *11*, 71–78. https://doi.org/10.1038/cmi.2013.43.

19. Castro, F., Cardoso, A.P., Gonçalves, R.M., Serre, K., and Oliveira, M.J. (2018). Interferon-Gamma at the Crossroads of Tumor Immune Surveillance or Evasion. Front. Immunol. *9*, 847. https://doi.org/10.3389/fimmu.2018.00847.

20. Sasaki, R., Kanda, T., Yokosuka, O., Kato, N., Matsuoka, S., and Moriyama, M. (2019). Exosomes and Hepatocellular Carcinoma: From Bench to Bedside. Int. J. Mol. Sci. *20*, 1406. https://doi.org/10.3390/ijms20061406.

21. Mimura, K., Teh, J.L., Okayama, H., Shiraishi, K., Kua, L.F., Koh, V., Smoot, D.T., Ashktorab, H., Oike, T., Suzuki, Y., et al. (2018). PD-L1 expression is mainly regulated by interferon gamma associated with JAK-STAT pathway in gastric cancer. Cancer Sci. *109*, 43–53. https://doi.org/10.1111/cas.13424.

22. Zhang, X., Zeng, Y., Qu, Q., Zhu, J., Liu, Z., Ning, W., Zeng, H., Zhang, N., Du, W., Chen, C., and Huang, J.A. (2017). PD-L1 induced by IFN-gamma from tumor-associated macrophages via the JAK/STAT3 and PI3K/AKT signaling pathways promoted progression of lung cancer. Int. J. Clin. Oncol. *22*, 1026–1033. https://doi.org/10.1007/s10147-017-1161-7.

23. Llovet, J.M., Castet, F., Heikenwalder, M., Maini, M.K., Mazzaferro, V., Pinato, D.J., Pikarsky, E., Zhu, A.X., and Finn, R.S. (2022). Immunotherapies for hepatocellular carcinoma. Nat. Rev. Clin. Oncol. *19*, 151–172. https://doi.org/10.1038/s41571-021-00573-2.

24. Li, C., Ni, Y.Q., Xu, H., Xiang, Q.Y., Zhao, Y., Zhan, J.K., He, J.Y., Li, S., and Liu, Y.S. (2021). Roles and mechanisms of exosomal non-coding RNAs in human health and diseases. Signal Transduct. Targeted Ther. *6*, 383. https://doi.org/10.1038/s41392-021-00779-x.

25. Zhang, Z., Yin, J., Lu, C., Wei, Y., Zeng, A., and You, Y. (2019). Exosomal transfer of long non-coding RNA SBF2-AS1 enhances chemoresistance to temozolomide in glioblastoma. J. Exp. Clin. Cancer Res. *38*, 166. https://doi.org/10.1186/s13046-019-1139-6.

26. Chen, Z., Chen, Y., Peng, L., Wang, X., and Tang, N. (2020). 2,5-dimethylcelecoxib improves immune microenvironment of hepatocellular carcinoma by promoting ubiquitination of HBx-induced PD-L1. J. Immunother. Cancer *8*, e001377. https://doi.org/10.1136/jitc-2020-001377.

27. Sun, Y., Yu, M., Qu, M., Ma, Y., Zheng, D., Yue, Y., Guo, S., Tang, L., Li, G., Zheng, W., et al. (2020). Hepatitis B virus-triggered PTEN/beta-catenin/c-Myc signaling enhances PD-L1 expression to promote immune evasion. Am. J. Physiol. Gastrointest. Liver Physiol. *318*, G162–G173. https://doi.org/10.1152/ajpgi.00197.2019.